Clinical, Cosmetic and Investigational Dermatology

Dovepress

open access to scientific and medical research

Open Access Full Text Article

ORIGINAL RESEARCH

Erzhiwan Ameliorates Restraint Stress- and Monobenzone-Induced Depigmentation in Mice by Inhibiting Macrophage Migration Inhibitory Factor and 8-Hydroxy-2-Deoxyguanosine

Nan Tang[1,*], Xiao-Ting Liu[2,*], Xiao-Li Lin[2], Wen-Xiu Yang[2], Qi-Lin Li[3], Guo-En Wang[2], Yan-Hua Wu[1]

[1]Departments of Traditional Chinese Medicine, Guangzhou Red Cross Hospital, Jinan University, Guangzhou, Guangdong, 510220, People's Republic of China; [2]School of Chinese Materia Medica, Guangdong Pharmaceutical University, Guangzhou, Guangdong, 510006, People's Republic of China; [3]Departments of Dermatology, Guangzhou Red Cross Hospital, Jinan University, Guangzhou, Guangdong, 510220, People's Republic of China

*These authors contributed equally to this work

Correspondence: Yan-Hua Wu, No. 396 Tongfu Zhong Road, Guangzhou, Guangdong Province, 510220, People's Republic of China, Email wuyanhua368@163.com; Guo-En Wang, No. 280, Waihuan East Road, University Town, Guangzhou, Guangdong Province, 510006, People's Republic of China, Email wangge07@126.com

Purpose: Vitiligo is an autoimmune disease that results in the loss of epidermal melanocytes. The treatments for patients with vitiligo remain lacking. Erzhiwan (EZW), a traditional Chinese Medicine composed of *Ligustri Lucidi Fructus* and *Ecliptae Herba*, was used to ameliorate depigmentation since ancient China. This study aims to investigate the effect of EZW on vitiligo-related depigmentation.

Methods: A vitiligo-related depigmentation mouse model was induced by monobenzone and restraint stress. The experimental depigmentation mice were treated with EZW. Histological observation of skin was conducted. Cutaneous oxidative damage and inflammation were determined. A network pharmacology analysis was carried out.

Results: EZW reduced depigmentation score ($p<0.01$), cutaneous inflammatory infiltration ($p<0.01$), and CD8α-positive expression ($p<0.01$), and increased cutaneous melanin content in experimental depigmentation mice. EZW reduced stress reaction in experimental depigmentation mice ($p<0.01$). EZW inhibited 8-hydroxy-2-deoxyguanosine (8-OHdG)-related DNA oxidative damage in the skin ($p<0.05$, $p<0.01$). In addition, EZW reduced cutaneous macrophage migration inhibitory factor (MIF)-CD74-NF-κB signaling ($p<0.01$). The network pharmacology analysis demonstrated that EZW regulated necroptosis, apoptosis, and FoxO signaling pathways in vitiligo. An in vitro experiment showed that the main ingredient of EZW, specnuezhenide, protected against monobenzone and MIF-induced cell death in HaCaT cells ($p<0.01$).

Conclusion: EZW ameliorates restraint stress- and monobenzone-induced depigmentation via the inhibition of MIF and 8-OHdG signaling. The findings provide a data basis of an utilization of EZW in vitiligo.

Keywords: vitiligo, 8-hydroxy-2-deoxyguanosine, *Ligustri Lucidi Fructus*, *Ecliptae Herba*, specnuezhenide

Introduction

Vitiligo is a relatively common autoimmune depigmenting disorder of the skin caused by the lack of skin melanocytes function or the decrease in the number of melanocytes.[1] The global prevalence of vitiligo is approximately 0.5–2%.[2] Reductions in beauty, self-esteem, and quality of life occur in patients with vitiligo.[3] Currently, the main treatments for vitiligo are non-labeled immunosuppressants, such as systemic or topical steroids, topical calcium-regulated neurophosphatase inhibitors, combined with the use of ultraviolet light.[4] In addition, drug candidates for ameliorating vitiligo include targeting the Janus kinase, and Wnt signaling, and microRNAs, or regulatory T cells.[5] However, the treatments for patients with vitiligo remain lacking.

Received: 13 June 2023
Accepted: 25 December 2023
Published: 22 January 2024

The Yin and Yang balance theory, originated from traditional Chinese Medicine (TCM), sums up that Erzhiwan (EZW), a prescription composed of *Ligustri Lucidi Fructus* and *Ecliptae Herba*, is used for the treatment of vitiligo. Cytokines status reflects the yin and yang of vitiligo pathogenesis. Different kinds of cytokines induce stress reaction, inflammation, and oxidative damage, thereby improving vitiligo development.[6] *Ligustri Lucidi Fructus* possesses various pharmacological effects, including hepatoprotective, antioxidant, immunomodulatory, and antiviral effects.[7] In addition, *Ecliptae Herba* has antioxidant, immunomodulatory, antibacterial, hypolipidemic, and hypoglycemic effects, and improves hair growth.[8] EZW reduces oxidative stress via increasing superoxide dismutase (SOD) activity and decreasing malondialdehyde (MDA) content, and inhibiting inflammatory cytokines including tumor necrosis factor-α, interleukin (IL)-1β, and IL-6.[9] Whether EZW ameliorates vitiligo remains unclear.

Stress is one of the factors involved in the pathogenesis of vitiligo.[10] Stress triggers an increase in $CD8^+$ T cells, and a decrease in $CD4^+$ T cells.[11] The level of macrophage migration inhibitory factor (MIF), a biomarker of vitiligo,[12] is increased in autoimmune hepatitis patients with psychological stress.[13] In addition, the level of 8-hydroxy-2 deoxyguanosine (8-OHdG), a biomarker of vitiligo,[14] is elevated by psychological stress treatments.[15] Previous reports indicate that the levels of vitiligo-related biomarkers including $CD8^+$ T cells, MIF, and 8-OHdG are increased in a depigmentation mouse model induced by monobenzone and restraint stress.[16] Considering that psychological stress affects the vitiligo-related cytokines, thereby breaking the Yin and Yang balance, this study hypothesizes that EZW ameliorates vitiligo. In this study, a restraint stress- and monobenzone-induced depigmentation mouse model was used to evaluate the amelioration of EZW. The underlying mechanism of EZW in vitiligo-related depigmentation was explored.

Materials and Methods

Animal Experiments and Treatments

Seven-week-old female C57BL/6 mice were purchased from Guangdong Medical Laboratory Animal Center (Guangdong, China). The hair of dorsum in an area of 2 × 2 cm^2 was removed by using a commercial depilated cream. To establish a depigmentation mice model, the depilated area was completely massaged with 40% monobenzone cream for 16 weeks. The control mice were treated with the base cream. The base cream was prepared as previously described.[16] Some monobenzone-induced mice were restrained in a ventilated 50 mL polypropylene tube for 18 h from 16:00 to the next day 10:00 every three days. The restraint stress treatments were continuously for 16 weeks.[16] Restraint stress- and monobenzone-treated mice were given with a subcutaneous injection of Cyclosporin A (CsA, 12.5 mg/kg) as a positive control.[17] Other restraint stress- and monobenzone-treated mice were orally administrated 2.57 g/kg of EZW every other day for the last 4 weeks. EZW, a decoction recorded in the Chinese Pharmacopoeia 2020 Edition, is composed of 9 g of *Ligustri Lucidi Fructus* and 9 g of *Ecliptae Herba*. The dosage of EZW (2.57 g/kg) contained 1.285 g/kg of *Ligustri Lucidi Fructus* extract and 1.285 g/kg of *Ecliptae Herba*, which was a conversion of the dose in mice from the clinical dose of EZW. The extracts of *Ligustri Lucidi Fructus* (Lot number A1065071) *and Ecliptae Herba* (Lot number A2011551) were from Guangdong E-Fong Pharmaceutical Co. Ltd. (Foshan, China). Each group included 10 mice. All the mice were maintained at 22 ± 2°C on a 12 h/12 h light/dark cycle. Animal experiment procedures were approved by the Institutional Animal Care Committee in Guangdong Pharmaceutical University as adopted and promulgated by the United States National Institutes of Health, and followed in a national standard of China (GB/T 35892–2018) for the ethical review of the welfare of laboratory animals (Animal experiment ethics approval number: gdpulacspf2017609).

The degree of depigmentation was quantified by two observers using a double-blind method as previously described.[16] In brief, the depigmentation areas in 75–100%, 50–75%, 25–50%, 10–25%, less than 10%, and 0 were recorded 5, 4, 3, 2, 1, and 0 score, respectively. The behavioral test was conducted by tail suspension test (TST), forced swimming test (FST), and open field test (OFT) as previously described.[16] In TST, mice were suspended with a tape 1 cm away from their tails and elevated 60 cm above the floor for 6 min. The immobile time was marked within the last 4 min. In FST, mice were placed in a plastic bucket (45 cm × 19 cm × 23 cm) filled with 25°C water

for 6 min. The resting time within the last 4 min was marked. In OFT, mice were placed in a 50 cm × 50 cm × 35 cm white box. The behaviors were recorded by a camera for 5 min. The moving distance and speed were calculated.

Histomorphology and Immunohistochemistry

After being fixed in 4% paraformaldehyde, the skin tissues were embedded in paraffin, and subsequently sliced into 3-μm sections. The samples were stained with hematoxylin and eosin or Masson-Fontana, respectively. Immunostaining on skin paraffin sections was performed with a SPlink detection kit (Biotin-Streptavidin HRP Detection systems, ZSGB-BIO, Beijing, China). Processed sections were performed with primary antibodies against nuclear factor-κB (NF-κB, 1:2000) and CD8a (1:2000, Abcam, USA). After washing with PBS for 3 times, the sections were incubated with their specific horseradish peroxidase-conjugated secondary antibodies for 1 h. Additionally, the nuclei of the skin samples were counterstained with hematoxylin. The morphological changes were observed using the Pannoramic MIDI (3D HISTEC, Hungary).

Terminal Deoxynucleotidyl Transferase dUTP Nick End Labeling (TUNEL) Staining

The 3-μm skin tissue sections were deparaffinized, rehydrated, and subjected to TUNEL staining with a TUNEL kit (Nanjing Jiancheng Bioengineering Institute, China). In brief, the TUNEL solution was dropped on the tissue sections and incubated for 60 min at 37°C away from light. The sections were washed for 3 times with PBS. Subsequently, the slices were sealed with an anti-fluorescence quenching sealing solution containing DAPI (Abcam, USA). The TUNEL-positive cells were observed under a fluorescence microscope IX73 (Olympus, Tokyo, Japan).

Immunofluorescence

After deparaffinization, antigen retrieval, and permeabilization, the 3-μm skin tissue sections were incubated with 3% H_2O_2 and blocked using 5% goat serum. Processed sections were performed with primary antibody against MIF (1:1000, Abcam, USA), CD74 (1:500, Santa Cruz, CA, USA), Melan-A (1:500), E-Cadherin (1:1000, Abcam, USA), arachidonate 15-lipoxygenase (ALOX15, 1:1000, Abcam, USA) and 8-OHdG (1:1000, Abcam, USA) at 4°C overnight, respectively. After washing with PBS for 3 times, the goat anti-rabbit antibody Alexa Fluor® 488 (1:1000, Abcam), goat anti-mouse antibody Alexa Fluor® 488 (1:1000, Abcam), and goat anti-rabbit antibody Alexa Fluor® 555 (1:1000, Abcam) were dropped into the section for incubation for 1 h at room temperature, respectively. DAPI (1:1000) was added in the sections for 10 min. After the above steps were completed, an appropriate amount of anti-fluorescence quenching sealing solution containing DAPI (Abcam, USA) was dropped onto the slices for sealing and drying. Fluorescence detection was conducted under the Pannoramic MIDI (3D HISTEC, Hungary).

Enzyme-Linked Immunosorbent Assay (ELISA)

The blood of mice was collected via puncture of the inner canthus. The samples were centrifuged at 13,200 × *g* for 10 min, and the supernatants were collected. The levels of MIF, 8-oxoguanine DNA glycosylase 1 (OGG1), and 8-OHdG were determined by using ELISA commercial kits (Jiangsu Mei Biao Biological Technology Co., Ltd., Jiangsu, China) in accordance with the manufacturer's instructions.

Quantitative Real-Time Polymerase Chain Reaction (RT-qPCR) Analysis

Total RNAs were isolated from the skin samples using the TRIZOL reagent (TaKaRa, Dalian, China), and reversely transcribed into cDNAs with the FastKing-RT SuperMix (Tiangen biotech, Beijing, China). PCR process was performed with a CFX Connect cyclerTM Real-Time system (Bio-Rad, Hercules, CA, USA) in presence of the THUNDERBIRD SYBR qPCR Mix (Toyobo, Osaka, Japan), cDNAs and specific primers. The primers included *Sod2* F: 5'-AGGACGGTGTGGCCAATGTG-3'and R: 5'-CGGCTCCCAGCATTTCCAGT-3'; *18S*: F: 5'-ACGGCTACCACATCC

-3' and R: 5'-CAGACTTGCCCTCCA-3'. Relative mRNA expression of each gene (relative to the ND group) was calculated by the delta cycle threshold method, and the results were normalized to the housekeeping gene *18S*.

Analysis of the Content of Specnuezhenide in EZW

The EZW powder sample (0.5 g) was extracted with 50 mL of 50% methanol using an ultrasonic method (40 kHz, 350 W) for 45 min. After centrifugation and filtration, the sample was prepared for determining specnuezhenide using high-performance liquid chromatography (HPLC, Agilent 1260 Infinity II, Agilent, Santa Clara, CA, USA) with the Welchrom C18 column (4.6 × 250 mm, 5-μm particle size) and the mobile phases consisted of methanol-water (64:36, v/v). The flow rate was 1 mL/min, and the wavelength of the UV detector was fixed at 224 nm. The content of specnuezhenide in EZW was calculated compared to the standard stock solution of specnuezhenide.

Cell Culture and Treatments

HaCaT cells were cultured in a DMEM medium containing 5% fetal bovine serum and 1% penicillin-streptomycin solution at 37°C and 5% CO_2. The HaCaT cell lines (300493, CLS cell bank, Germany) were purchased from Shanghai Jinyuan Biotechnology Co., Ltd (Lot: JY051). The cells (1×10^3) were incubated 400 μM monobenzone and 10 ng/mL MIF,[18,19] and incubated with or without specnuezhenide (12.5, 25, or 50 μM) for 24 h. The MIF inhibitor, ISO-1 (10 μM), was used as a positive control. After 24 h, 25 μL MTT solution (5 mg/mL) was added to each well and incubated 4 h. After 4 h, the supernatants were discarded, and 150 μL DMSO solutions were added to the cells for 10-min incubation. The cell viability was calculated by detecting the absorbance value at 570 nm.

Network Pharmacology Analysis

The main chemical components of EZW were collected from CNKI (www.cnki.net) and PubMed (https://www.ncbi.nlm.nih.gov/pmc) databases. The molecular structure of components was collected by PubChem (http://pubchem.ncbi.nlm.nih). The PharmMapper (https://www.nc-bi.nlm.nih.gov/pmc) and TCMSP (https://www.ncbi.nlm.nih.gov/pmc) databases were used to predict and collect target proteins.[20] When the identified proteins were searched in the UniProt database (https://www.uniprot.org), 1022 and 1270 relevant targets were obtained from the GeneCard database (https://www.genecards.org/) via input of "oxidative stress" and "Vitiligo", respectively. Networks of functional enrichment terms generated using the MetaScape database (http://metascape.org) were visualized in Cytoscape (https://cytoscape.org). The top 20 pathways screened by KEGG enrichment analysis under the condition of $p<0.05$ were imported into Hilpot platform for visual processing.[21]

Statistical Analysis

Data are presented as mean ± standard deviation (SD). One-way analysis of variance followed by a post hoc analysis with Newman–Keuls multiple comparison test or Tukey's multiple comparison test was used to analyze the difference in the groups using GraphPad Prism 8.0 (GraphPad Software, Inc.). And $p<0.05$ was considered a significant difference.

Results

EZW Reduced Skin Depigmentation in Restraint Stress- and Monobenzone-Treated Mice

A depigmentation mouse model induced by restraint stress and monobenzone was administrated EZW and CsA (Figure 1A). Ddepigmentation score and cutaneous inflammatory infiltration were increased, and cutaneous melanin content were decreased in the restraint stress- and monobenzone-treated mice, compared with that of the monobenzone-treated mice (Figure 1, $p<0.01$). EZW decreased depigmentation score ($p<0.01$) and cutaneous inflammatory infiltration ($p<0.01$) and increased cutaneous melanin content in depigmentation mice (Figure 1B–D). EZW reversed the increase in cutaneous CD8α-positive expression in the depigmentation mice (Figure 1E, $p<0.01$). In addition, the level of co-localization of Melan-A and E-Cadherin was increased in depigmentation mice with EZW

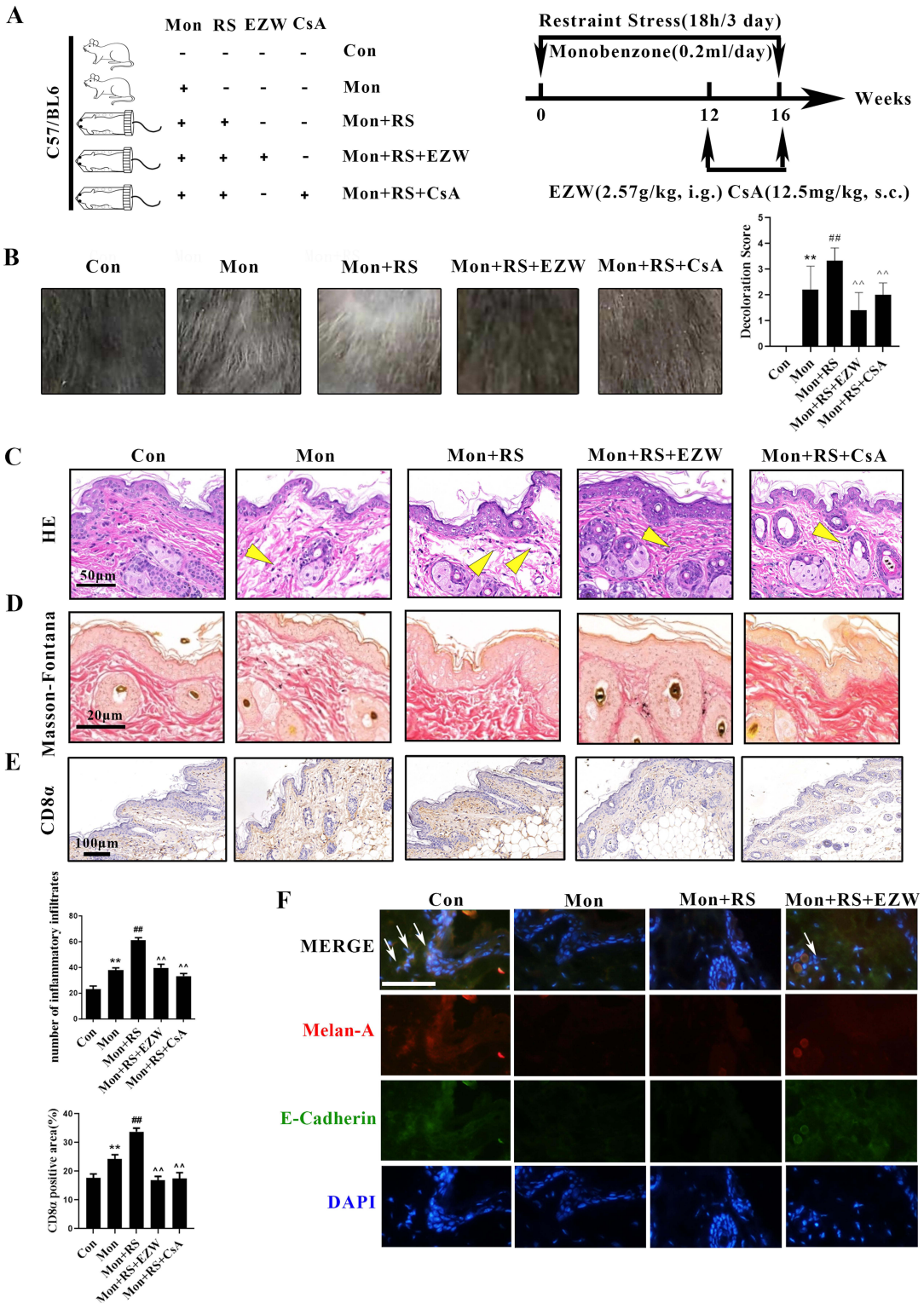

Figure 1 Erzhiwan reduced skin depigmentation in restraint stress- and monobenzone-treated mice. (**A**) The process of restraint stress- and monobenzone-induced depigmentation in mice and the treatments were shown. (**B**) Representative images of depigmentation in the dorsum were shown, and the depigmentation score in each group was evaluated (n=10). (**C**) H&E staining were conducted. The inflammatory infiltration was marked with yellow arrows (n=3). Scale bar=50 μm. (**D**) Masson-Fontana staining was carried out to observe melanin content. The melanin was stained with black. Scale bar=20 μm. (**E**) CD8α-positive expression was detected using an immunohistochemistry method (n=3). The expression was stained with brown. Scale bar=100 μm. (**F**) The immunofluorescence double staining was used to determine the co-localization of Melan-A (Red) and E-Cadherin (Green) with white arrows. Nuclei were stained with DAPI (Blue). Scale bar=50 μm. Data are expressed as mean ± SD, and compared with Con group at ** $p < 0.01$, and compared with Mon group at $^{\#\#}p < 0.01$, and compared with Mon+RS group at $^{\wedge\wedge}p < 0.01$.

Abbreviations: Con, the control mice; Mon, monobenzone-treated mice; Mon+RS, monobenzone- and restraint stress-treated mice; Mon+RS+EZW, monobenzone- and restraint stress-treated mice administrated Erzhiwan; Mon+RS+CsA, monobenzone- and restraint stress-treated mice administrated cyclosporin A.

treatments (Figure 1F). The data indicated that EZW reduced CD8α-positive immune cells and protected melanocytes in the experimental depigmentation mice.

EZW Decreased Stress Reaction in Experimental Depigmentation Mice

The behavioral test demonstrated that an increase in immobile time of TST and FST, and a decrease in speed and total distance of OFT were observed in depigmentation mice ($p<0.01$). EZW reduced the immobile time of TST and FST, and increased speed and total distance of OFT in experimental depigmentation mice (Figure 2, $p<0.01$). Thus, EZW reduced the stress-related behaviors. It suggested that EZW decreased stress reaction in experimental depigmentation mice.

EZW Reduced DNA Oxidative Damage in Experimental Depigmentation Mice

TUNEL staining data demonstrated that the level of TUNEL-positive cells in the skin was increased in the depigmentation mice. EZW reduced the level of TUNEL-positive cells in the skin (Figure 3A). In addition, EZW inhibited the expression of cutaneous 8-OHdG (Figure 3B) and decreased plasma 8-OHdG content (Figure 3D, $p<0.01$). EZW inhibited cutaneous ALOX15-positive expression (Figure 3C) and increased cutaneous *Sod2* mRNA expression (Figure 3E, $p<0.05$) and plasma OGG1 content (Figure 3F, $p<0.01$) in experimental depigmentation mice. Thus, EZW reduced cutaneous DNA oxidative damage.

EZW Downregulated the MIF-CD74-NF-κB Signaling in Experimental Depigmentation Mice

Further investigation showed that EZW reversed the increases in MIF-positive expression in the skin (Figure 4A) and MIF content in the plasma (Figure 4B, $p<0.01$) in experimental depigmentation mice. The co-localization of MIF and CD74 was reduced in experimental depigmentation mice with EZW treatments (Figure 4C). In addition, EZW inhibited nuclear NF-κB-positive expression in the skin in experimental depigmentation mice (Figure 4D). The data indicated that EZW downregulated the MIF-CD74-NF-κB signaling.

Network Pharmacology Analysis Demonstrated That EZW Reduced Oxidative Damage

The result of network pharmacology analysis found that 74 targets and 18 signaling pathways of EZW ameliorating vitiligo were obtained by using KEGG analysis. The signaling pathways of EZW targeting oxidative damage and vitiligo involved the necroptosis, apoptosis, and FoxO signaling pathways (Figure 5A). The main ingredients of EZW are linked to SOD2, MIF, CCL5, ARG1, JAK3, and IL-2. A network of active ingredients-targets-signaling pathways is shown in

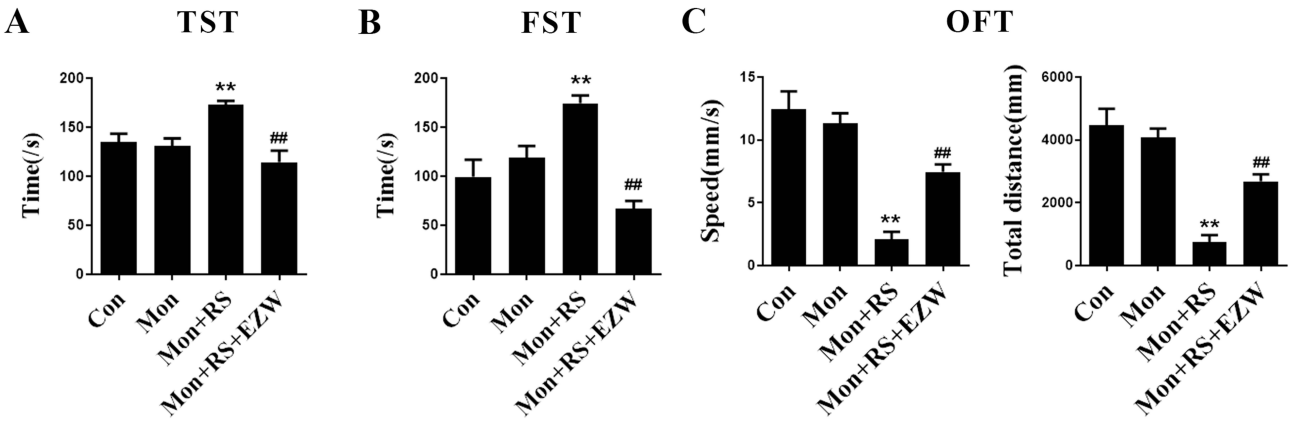

Figure 2 Erzhiwan decreased stress reaction in experimental depigmentation mice. The immobile time of TST (**A**) and FST (**B**) of the mice was detected. (**C**) OFT analysis of the mice was performed (n=8). Data are expressed as mean ± SD, and compared with Mon group at $^{**}p < 0.01$, and compared with Mon+RS group at $^{\#\#}p < 0.01$.
Abbreviations: Con, the control mice; Mon, monobenzone-treated mice; Mon+RS, monobenzone- and restraint stress-treated mice; Mon+RS+EZW, monobenzone- and restraint stress-treated mice administrated Erzhiwan; TST, tail suspension test; FST, forced swimming test; OFT, open field test.

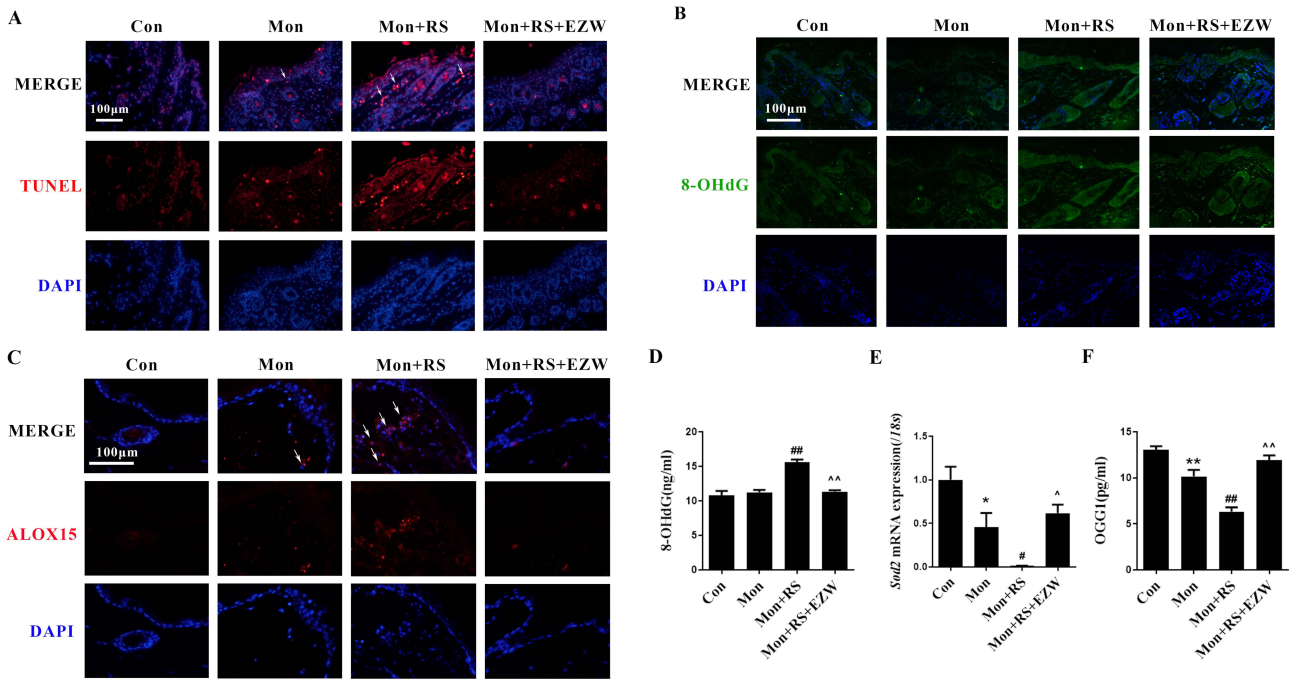

Figure 3 Erzhiwan reduced DNA oxidative damage in experimental depigmentation mice. (**A**) TUNEL staining was used to observe the level of apoptosis in the skin. The TUNEL-positive cells were marked with white arrows. Scale bar=100 μm. The expression of 8-OHdG (**B**) and ALOX15 (**C**) in the skin was detected using an immunofluorescence method. The expression was marked with white arrows. Scale bar=100 μm. (**D**) The level of plasma 8-OHdG was detected using an ELISA method (n=6). (**E**) The mRNA expression of *Sod2* was detected (n=3). (**F**) Plasma OGG1 content was detected using an ELISA method (n=6). Data are expressed as mean ± SD, and compared with Con group at $^{*}p < 0.05$ and $^{**}p < 0.01$, and compared with Mon group at $^{\#}p < 0.05$ and $^{\#\#}p < 0.01$, and compared with Mon+RS group at $^{\wedge}p < 0.05$ and $^{\wedge\wedge}p < 0.01$.

Abbreviations: Con, the control mice; Mon, monobenzone-treated mice; Mon+RS, monobenzone- and restraint stress-treated mice; Mon+RS+EZW, monobenzone- and restraint stress-treated mice administrated Erzhiwan.

Figure 5B. The content of specnuezhenide, one of the main ingredients in *Ligustri Lucidi Fructus* in EZW, was 5.229 mg/g (Figure 5C). The in vitro data showed that 12.5, 25, and 50 μM specnuezhenide reversed the decrease in cell viability in monobenzone- and MIF-treated HaCaT cells ($p<0.01$). In addition, specnuezhenide failed to improve cell viability in monobenzone- and MIF-treated HaCaT cells when compared with MIF inhibitors (Figure 5D). Therefore, the amelioration of EZW on oxidative damage involved the MIF signaling.

Discussion

EZW is a prescription for the treatment of Liver and Kidney deficiency according to the TCM theory. In China, the expert consensus recommended EZW for the treatment of vitiligo. Vitiligo is characterized by progressive depigmentation by the loss of melanocytes, activation of $CD8^+$ T lymphocytes, and increases in MIF and 8-OHdG levels.[11,12,14] In this study, we verified that EZW reduced depigmentation score and cutaneous inflammatory infiltration, and increased melanin content in restraint stress- and monobenzone-induced depigmentation in mice. In addition, EZW inhibited cutaneous CD8α-positive expression, and reduced the levels of cutaneous MIF and 8-OHdG. In this experiment, few side effects have been found in EZW-treated mice, in accordance with the previous acute toxic evaluation showing that few significant changes were observed in body weight or physiological status with an oral dose of 60 g/kg of EZW in mice.[22] According to the findings above, EZW is regarded as one of the promising options for the treatment of vitiligo.

Activation of $CD8^+$ T cells triggers the destruction of melanocytes in vitiligo.[23] Our current data demonstrated that EZW inhibited the expression of cutaneous CD8α and reduced the level of stress reaction in experimental depigmentation mice. In addition, the damage of melanocytes induces a destabilization of the basal layer of epidermis in patients with vitiligo, accompanied by a decrease in plasma SOD content[24] and increases in levels of MDA and 8-OHdG.[14] In this study, EZW reduced the level of apoptosis via the increases in expressions of SOD and OGG1, and decreases in

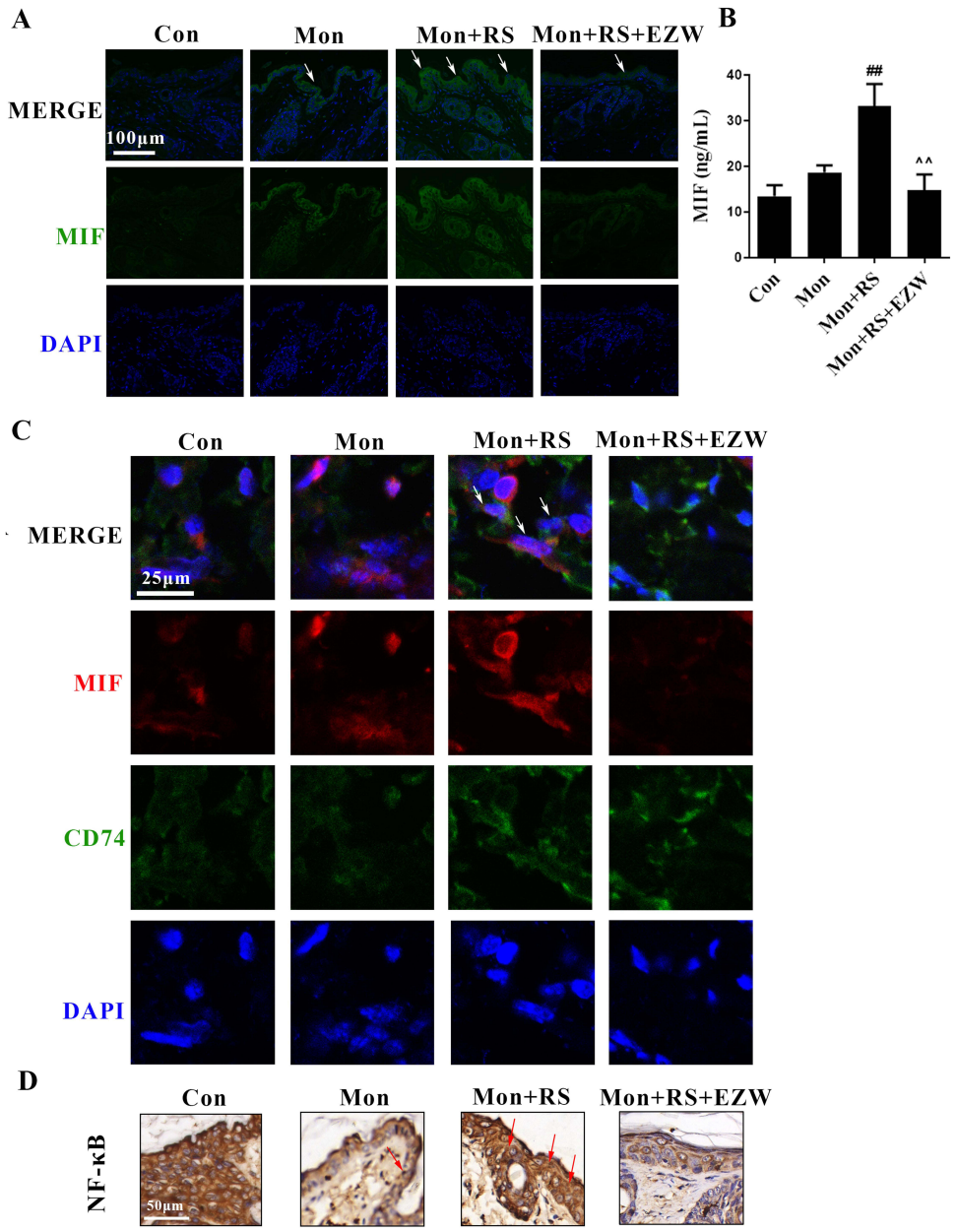

Figure 4 Effects of Erzhiwan on the MIF-CD74-NF-κB signal in experimental depigmentation mice. (**A**) MIF-positive expression in the skin was determined using an immunofluorescence method, and marked with white arrows. Scale bar=100 μm. (**B**) Plasma MIF content was detected using an ELISA method (n=6). (**C**) The immunofluorescence double staining was used to determine the co-localization of MIF and CD74, and the co-localization was marked with white arrows. Scale bar=25 μm. (**D**) Nuclear NF-κB-positive expression was detected using an immunohistochemical method, and the expression was marked with red arrows. Scale bar=50 μm. Data are expressed as mean ± SD, and compared with Mon group at $^{\#\#}p < 0.01$, and compared with Mon+RS group at $^{\wedge\wedge}p < 0.01$.

Abbreviations: Con, the control mice; Mon, monobenzone-treated mice; Mon+RS, monobenzone- and restraint stress-treated mice; Mon+RS+EZW, monobenzone- and restraint stress-treated mice administrated Erzhiwan.

expressions of 8-OHdG and ALOX15. OGG1 repairs DNA by targeting 8-OHdG.[25] ALOX15 promotes lipid peroxidation, and triggers ferroptosis.[26] Thus, EZW ameliorates vitiligo-related depigmentation via the inhibition of epidermal oxidative damage. Furthermore, CD74, one of the receptors of MIF,[27] upregulates NF-κB activation.[28] EZW decreased the transcription of NF-κB into the nucleus via the reduction of MIF expression and the co-localization of MIF and CD74. Therefore, EZW helped to balance the Yin and Yang problem of vitiligo through inhibiting stress reaction, inflammation, and oxidative damage.

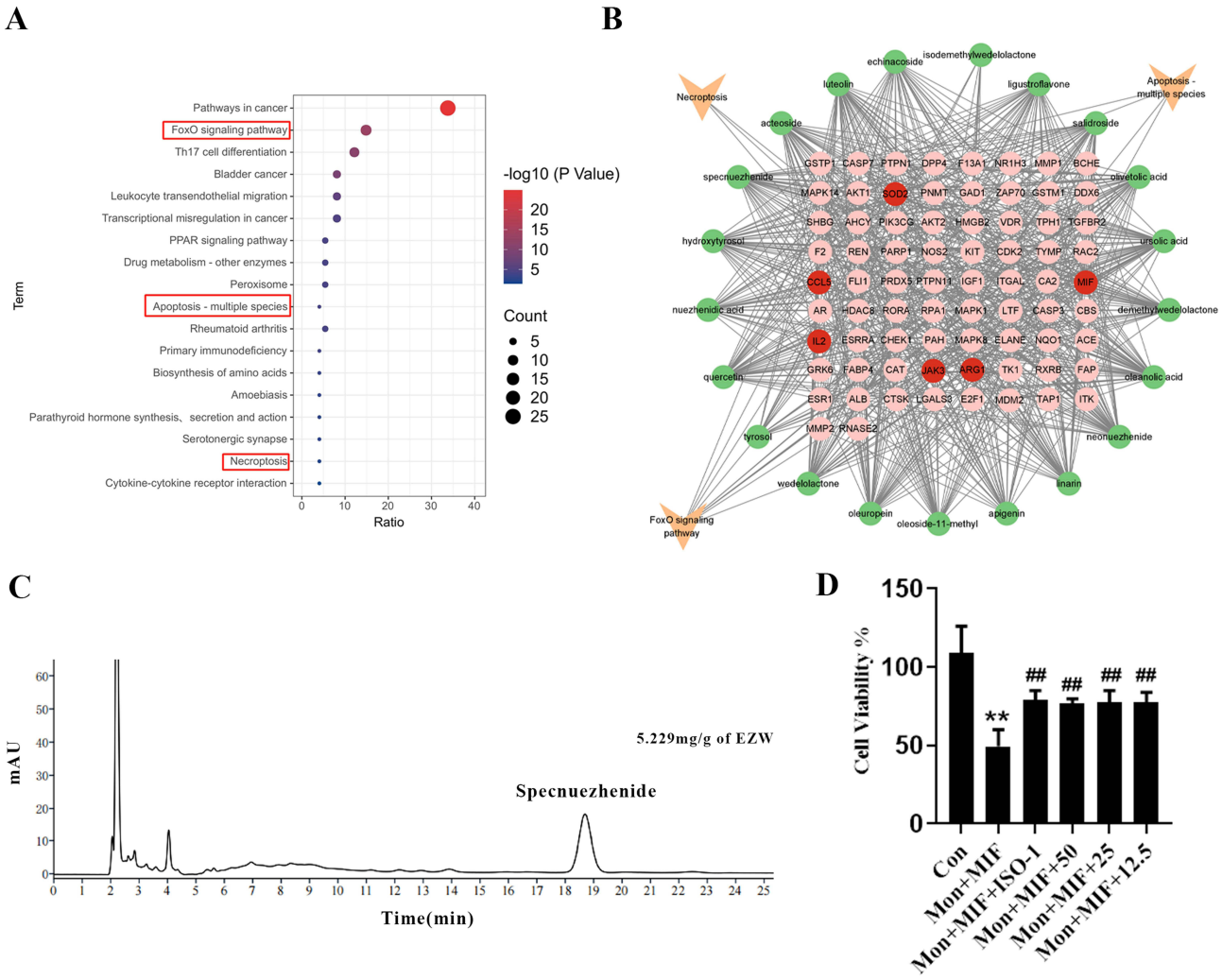

Figure 5 Network pharmacology analysis demonstrated that specnuezhenide inhibited oxidative damage in vitiligo. (**A**) The KEGG pathway analysis was shown. The key pathways were circled by red rectangles. (**B**) The active ingredients-targets-signaling pathways network was shown. Green circles represented the main ingredients of Erzhiwan. The pink or red circles represented the targets. Orange arrows represented the predicted signaling pathways. (**C**) HPLC analysis of Erzhiwan was carried out with a wavelength of 224 nm. The peak was specnuezhenide. (**D**) HaCaT cells were treated with monobenzone and MIF. Cell viability was determined using a MTT assay (n=6). Data are expressed as mean ± SD, and compared with Con group at $^{**}p < 0.01$, and compared with Mon+MIF group at $^{\#\#}p < 0.01$.

Abbreviations: Con, the control HaCaT cells. Mon+MIF: monobenzone- and MIF-induced HaCaT cells; Mon+MIF+ISO-1, Mon+MIF cells treated with 10 μM ISO-1. Mon+MIF+50: Mon+MIF cells treated with 50 μM specnuezhenide; Mon+MIF+25, Mon+MIF cells treated with 25 μM specnuezhenide; Mon+MIF+12.5, Mon+MIF cells treated with 12.5 μM specnuezhenide.

Network pharmacology analysis demonstrated that EZW, composed of *Ligustri Lucidi Fructus* and *Ecliptae Herba*, inhibited oxidative damage in vitiligo via the necroptosis, apoptosis, and FoxO signaling pathways. Previous studies showed that specnuezhenide, one of the main ingredients in EZW, reduces liver injury in mice by inhibiting oxidative stress and apoptosis, and inhibits NF-κB signaling.[29,30] An in vitro model of HaCaT cells induced by monobenzone and MIF[16] was used to evaluate the effect of specnuezhenide on oxidative damage. The results found that specnuezhenide protected against monobenzone- and MIF-induced oxidative damage in HaCaT keratinocytes. Another ingredient of *Ligustri Lucidi Fructus*, echinacoside, directly binds to SIRT1 and regulates FoxO expression to enhance autophagy in the neurons.[31] Small amounts of oleanolic acids in *Ligustri Lucidi Fructus* have anti-inflammatory and antioxidant effects.[32] The oleanolic acids modulate the nuclear localization of FoxO.[33] In addition, one main ingredient of *Ecliptae Herba*, wedelolactone, inhibits apoptosis, autophagy, and inflammasome activation.[34,35] The findings of main ingredients of EZW supported that EZW ameliorated vitiligo-related depigmentation via the inhibition of inflammation and oxidative damage.

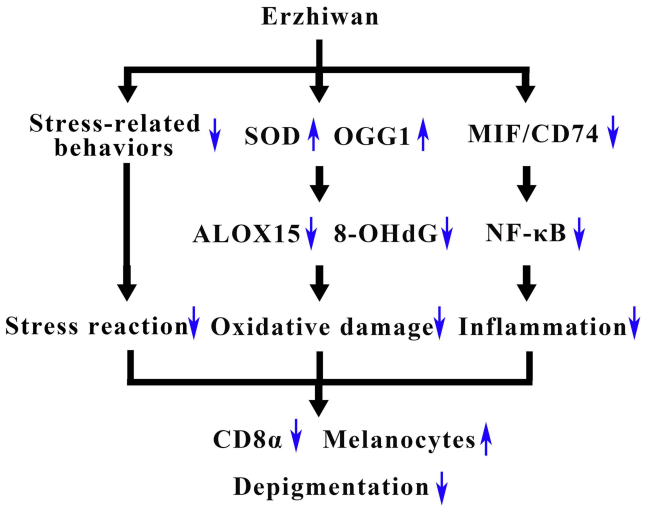

Figure 6 Schematic graph of the mechanism of Erzhiwan on restraint stress- and monobenzone-induced depigmentation in mice.

In conclusion, EZW ameliorates restraint stress- and monobenzone-induced depigmentation in mice via the inhibition of the MIF and 8-OHdG (Figure 6). The findings may provide a data basis of the utilization of EZW in vitiligo.

Data Sharing Statement

The data used to support the findings of this study are available from the corresponding authors upon request.

Acknowledgments

This work was supported by Guangdong Basic and Applied Basic Research Foundation [grant numbers 2019A1515010633, 2023A1515011701], and Construction Project of Synergistic Therapy of Traditional Chinese and Western Medicine on Major and Difficult Problems of Diseases in Guangzhou, and Construction Project of Three-grade Inheritance Studio of Famous Traditional Chinese Medicine Practitioner in Guangzhou [grant number 3 of Suiweizhongyi (2022)], and Guangzhou Municipal Science and Technology Project, China [grant number 202102020766], and Guangzhou Traditional Chinese Medicine and Integrated Traditional and Western Medicine Science and Technology Project [grant number 20232A011007], and Innovative Team Project of Ordinary Universities in Guangdong Province [grant number 2022KCXTD016].

Author Contributions

All authors made substantial contributions to conception and design, acquisition of data, or analysis and interpretation of data; took part in drafting the article or revising it critically for important intellectual content; agreed to submit to the current journal; gave final approval of the version to be published; and agree to be accountable for all aspects of the work.

Disclosure

The authors declare that there is no conflict of interest regarding the publication of this article.

References

1. Pei T, Zheng C, Huang C, et al. Systematic understanding the mechanisms of vitiligo pathogenesis and its treatment by qubaibabuqi formula. *J Ethnopharmacol*. 2016;190:272–287. doi:10.1016/j.jep.2016.06.001
2. Wang Y, Li S, Li C. Clinical features, immunopathogenesis, and therapeutic strategies in vitiligo. *Clin Rev Allergy Immunol*. 2021;61(3):299–323. doi:10.1007/s12016-021-08868-z
3. Huraib GB, Al Harthi F, Arfin M, Aljamal A, Alrawi AS, Al-Asmari A. Association of functional polymorphism in protein tyrosine phosphatase nonreceptor 22 (PTPN22) gene with vitiligo. *Biomark Insights*. 2020;15:1177271920903038. doi:10.1177/1177271920903038

4. Migayron L, Boniface K, Vitiligo SJ. From physiopathology to emerging treatments: a review. *Dermatol Ther*. 2020;10(6):1185–1198. doi:10.1007/s13555-020-00447-y
5. Feng Y, Lu Y. Advances in vitiligo: update on therapeutic targets. *Front Immunol*. 2022;13:986918. doi:10.3389/fimmu.2022.986918
6. Singh M, Kotnis A, Jadeja SD, et al. Cytokines: the yin and yang of vitiligo pathogenesis. *Expert Rev Clin Immunol*. 2019;15(2):177–188. doi:10.1080/1744666X.2019.1550358
7. Pang Z, Zhi-yan Z, Wang W, et al. The advances in research on the pharmacological effects of fructus ligustri lucidi. *Biomed Res Int*. 2015;2015:281873. doi:10.1155/2015/281873
8. Timalsina D, Devkota HP. Eclipta prostrata (L.) L. (Asteraceae): ethnomedicinal uses, chemical constituents, and biological activities. *Biomolecules*. 2021;11(11):1738. doi:10.3390/biom11111738
9. Tang G, Li S, Zhang C, et al. Clinical efficacies, underlying mechanisms and molecular targets of Chinese medicines for diabetic nephropathy treatment and management. *Acta Pharm Sin B*. 2021;11(9):2749–2767. doi:10.1016/j.apsb.2020.12.020
10. Harris JE. Cellular stress and innate inflammation in organ-specific autoimmunity: lessons learned from vitiligo. *Immunol Rev*. 2016;269(1):11–25. doi:10.1111/imr.12369
11. Masafi S, Saadat SH, Tehranchi K, et al. Effect of stress, depression and type d personality on immune system in the incidence of coronary artery disease. *Open Access Maced J Med Sci*. 2018;6(8):1533–1544. doi:10.3889/oamjms.2018.217
12. Garcia-Orozco A, Martinez-Magaña IA, Riera-Leal A, et al. Macrophage inhibitory factor (MIF) gene polymorphisms are associated with disease susceptibility and with circulating MIF levels in active non-segmental vitiligo in patients from western Mexico. *Mol Genet Genomic Med*. 2020;8(10):e1416. doi:10.1002/mgg3.1416
13. Alrabadi LS, Dutton A, Rabiee A, et al. Mindfulness-based stress reduction may decrease stress, disease activity, and inflammatory cytokine levels in patients with autoimmune hepatitis. *JHEP Rep*. 2022;4(5):100450. doi:10.1016/j.jhepr.2022.100450
14. Li SL, Dai W, Wang SJ, et al. Clinical significance of serum oxidative stress markers to assess disease activity and severity in patients with non-segmental vitiligo. *Front Cell Dev Biol*. 2021;9:739413. doi:10.3389/fcell.2021.739413
15. Colaianna M, Schiavone S, Zotti M, et al. Neuroendocrine profile in a rat model of psychosocial stress: relation to oxidative stress. *Antioxid Redox Signal*. 2013;18(12):1385–1399. doi:10.1089/ars.2012.4569
16. Tang N, Liu XT, Wen WL, et al. Restraint stress promotes monobenzone-induced depigmentation in mice via the activation of glucocorticoid receptor/macrophage migration inhibitory factor signaling pathway. *Mol Immunol*. 2023;161:33–43. doi:10.1016/j.molimm.2023.07.007
17. Mehta H, Kumar S, Parsad D, et al. Oral cyclosporine is effective in stabilizing active vitiligo: results of a randomized controlled trial. *Dermatol Ther*. 2021;34(5):e15033. doi:10.1111/dth.15033
18. van den Boorn JG, Konijnenberg D, Tjin EP, et al. Effective melanoma immunotherapy in mice by the skin-depigmenting agent monobenzone and the adjuvants imiquimod and CpG. *PLoS One*. 2010;5(5):e10626. doi:10.1371/journal.pone.0010626
19. Schrader J, Deuster O, Rinn B, et al. Restoration of contact inhibition in human glioblastoma cell lines after MIF knockdown. *BMC Cancer*. 2009;9(1):464. doi:10.1186/1471-2407-9-464
20. Han J, Hou J, Liu Y, et al. Using network pharmacology to explore the mechanism of panax notoginseng in the treatment of myocardial fibrosis. *J Diabetes Res*. 2022;2022:8895950. doi:10.1155/2022/8895950
21. Pan HT, Xi ZQ, Wei XQ, et al. A network pharmacology approach to predict potential targets and mechanisms of "ramulus cinnamomi (cassiae) – Paeonia lactiflora" herb pair in the treatment of chronic pain with comorbid anxiety and depression. *Ann Med*. 2022;54(1):413–425. doi:10.1080/07853890.2022.2031268
22. Xie YY, Yan B, Hou M, et al. Erzhi pills ameliorate cognitive dysfunction and alter proteomic hippocampus profiles induced by d-galactose and aβ 1–40 injection in ovariectomized alzheimer's disease model rats. *Pharm Biol*. 2021;59(1):1402–1414. doi:10.1080/13880209.2021.1990353
23. Berbert Ferreira S, Berbert Ferreira R, Neves Neto AC, et al. Topical tofacitinib: a janus kinase inhibitor for the treatment of vitiligo in an adolescent patient. *Case Rep Dermatol*. 2021;13(1):190–194. doi:10.1159/000513938
24. Tuna A, Ozturk G, Gerceker TB, et al. Superoxide dismutase 1 and 2 gene polymorphism in Turkish vitiligo patients. *Balkan J Med Genet*. 2017;20(2):67–73. doi:10.1515/bjmg-2017-0033
25. Chen LY, Wang Y, Terkeltaub R, et al. Activation of AMPK-SIRT3 signaling is chondroprotective by preserving mitochondrial DNA integrity and function. *Osteoarthritis Cartilage*. 2018;26(11):1539–1550. doi:10.1016/j.joca.2018.07.004
26. Snodgrass RG, Benatzy Y, Schmid T, et al. Efferocytosis potentiates the expression of arachidonate 15-lipoxygenase (ALOX15) in alternatively activated human macrophages through LXR activation. *Cell Death Differ*. 2021;28(4):1301–1316. doi:10.1038/s41418-020-00652-4
27. Le Hiress M, Tu L, Ricard N, et al. Proinflammatory signature of the dysfunctional endothelium in pulmonary hypertension. role of the macrophage migration inhibitory factor/CD74 complex. *Am J Respir Crit Care Med*. 2015;192(8):983–997. doi:10.1164/rccm.201402-0322OC
28. Li W, Sultana N, Yuan L, et al. CD74 in apoptotic macrophages is associated with inflammation, plaque progression and clinical manifestations in human atherosclerotic lesions. *Metabolites*. 2022;12(1):54. doi:10.3390/metabo12010054
29. Hu D, Huang S, Ding Y, et al. Specnuezhenide reduces carbon tetrachloride-induced liver injury in mice through inhibition of oxidative stress and hepatocyte apoptosis. *J Pharm Pharmacol*. 2022;74(2):191–199. doi:10.1093/jpp/rgab164
30. Wang QQ, Han S, Li XX, et al. Nuezhenide exerts anti-inflammatory activity through the NF-κB pathway. *Curr Mol Pharmacol*. 2021;14(1):101–111. doi:10.2174/1874467213666200611141337
31. Yin R, Xue J, Tan Y, et al. The positive role and mechanism of herbal medicine in parkinson's disease. *Oxid Med Cell Longev*. 2021;2021:9923331. doi:10.1155/2021/9923331
32. Nyakudya TT, Mukwevho E, Erlwanger KH. The protective effect of neonatal oral administration of oleanolic acid against the subsequent development of fructose-induced metabolic dysfunction in male and female rats. *Nutr Metab*. 2018;15(1):82. doi:10.1186/s12986-018-0314-7
33. Proshkina E, Plyusnin S, Babak T, et al. Terpenoids as potential geroprotectors. *Antioxidants*. 2020;9(6):529. doi:10.3390/antiox9060529
34. Wang XQ, Liu RP, Wang J, et al. Wedelolactone facilitates the early development of parthenogenetically activated porcine embryos by reducing oxidative stress and inhibiting autophagy. *PeerJ*. 2022;10:e13766. doi:10.7717/peerj.13766
35. Pan H, Lin Y, Dou J, et al. Wedelolactone facilitates ser/thr phosphorylation of NLRP3 dependent on PKA signalling to block inflammasome activation and pyroptosis. *Cell Prolif*. 2020;53(9):e12868. doi:10.1111/cpr.12868